[AMERICAN JOURNAL OF SCIENCE, VOL. 274, NOVEMBER, 1974, P. 961-986]

American Journal of Science

NOVEMBER 1974

THEORETICAL PREDICTION OF EQUILIBRIUM PHASE ASSEMBLAGES IN MULTICOMPONENT SYSTEMS

THOMAS H. BROWN* and BRIAN J. SKINNER

Department of Geology and Geophysics, Yale University, New Haven, Connecticut 06520

ABSTRACT. Previous methods used to compute equilibrium phase assemblages have been restricted by the limited number of phases and components which could be considered in a calculation time that is economically feasible. Thermodynamic equations are here derived for the rapid calculation of equilibrium phase assemblages in large (>15) component systems with provision for n-end member non-ideal solution phases. Computer evaluation of these equations permits prediction of the identity of the stable phases as well as their relative masses for any chosen temperature, pressure, and bulk composition. With the thermodynamic data and computers presently available equilibrium phase assemblage calculations can be carried out to aid in the interpretation and evaluation of experimental data and field observations as well as to check on the internal consistency of the thermodynamic data. Examples of computations are presented in part 2 for both igneous and metamorphic rocks.

PART 1. THERMODYNAMIC RELATIONS

INTRODUCTION

It is evident from classical thermodynamics that for any system of known bulk composition, we need only know the thermodynamic properties of all possible phases that can exist in the system in order to identify the presence, composition, and masses of phases coexisting in equilibrium under any set of physical constraints (such as temperature, pressure, volume, open or closed system) we may choose to specify. Though simple to state, the operations involved in identifying an equilibrium assemblage (by which we mean the most stable assemblage) in a multicomponent system are not straightforward. It is the purpose of part 1 of this communication to lay the groundwork for our attempt to carry out this process. We therefore present first a summary of the thermodynamic principles, definitions, and relations pertinent to the calculation of equilibrium phase assemblages. Part 2 deals with the application of our calculations to certain geologic problems and observations. For readers who do not wish to work through the principles, part 2 has been written as an essentially separate document.

The problem of identifying an "equilibrium" assemblage is an old one in geology — particularly in igneous petrology, where it has been most helpful to compute mineral "assemblages" for a range of bulk compositions. One of the earliest and most successful attempts is due to Cross and others (1903) who devised the well-known CIPW normative

* Present address: Department of Geological Sciences, University of British Columbia, Vancouver 8, British Columbia, Canada

calculations. Their method is restricted to a small region of temperature, pressure, and compositional space but nevertheless makes indirect use of thermodynamics in calculating an "equilibrium" assemblage. This indirect use arises because of the employment of known universal compatibilities, which are in turn a measure of the relative Gibbs free energy between the phases considered. Execution of a CIPW norm to determine the relative masses of phases present in the "equilibrium" assemblage involves the solution of a set of simultaneous linear equations in which masses of components are distributed among a pre-selected group of phases.

The calculation of an equilibrium assemblage of coexisting phases, including solution phases, should not be confused with "chemical equilibria" computations. The determination of "chemical equilibria" from thermodynamic data involves the calculation of the distribution of species in one solution phase, usually a gas or aqueous solution in geologic circumstances, and can provide for inclusion of other phases. The numerical procedures used to calculate the various equilibrium distributions of species in complex solution phases have been summarized by Van Zeggeren and Storey (1970). These procedures are not, in general, applicable to the computation of equilibrium phase assemblages.

Previous attempts (for example, Brown, ms) to compute equilibrium assemblages from bulk composition and thermodynamic data have been based on free energy minimization techniques. This involves computing all possible phase assemblages to determine the one assemblage with the lowest Gibbs free energy. Even if large third generation computers are used and we ignore the complexities introduced by solution phases, the computation times required in these schemes is prohibitive for problems of geologic interest. For example, a system containing 12 components and 45 possible phases will generate approximately 3×10^{10} combinations. In general, this "brute force" procedure is not economically feasible for (>10) component systems. We have, therefore, developed a computation method that greatly restricts the calculation time required and that further allows us the option of considering solid solution among the phases present.

Before developing the conceptual and mathematical procedure used in this study to compute equilibrium assemblages, we will discuss the formal thermodynamic reasoning that allows an equilibrium assemblage to be computed once the bulk composition, temperature, and pressure are specified. In the following discussions, it should be noted that only *isothermal-isobaric closed systems* are considered.

DUHEM'S THEOREM

The thermodynamic relations that allow calculation of an equilibrium phase assemblage from a bulk composition at a specified temperature and pressure for a closed system are based on *Duhem's theorem* (Duhem, 1899; Prigogine and Defay, 1954, p. 187-189). *Duhem's theorem* addresses itself to the number of independent variables that must be

specified to determine completely the equilibrium state of a closed system. Both the extensive and intensive variables characterizing each phase must be known in order to determine completely the equilibrium state of the system.

In a system of C components, the total number of independent parameters in a system is C + 2. If the bulk composition of the system is given (that is, the mass of each component) then C additional parameters are specified, and only two variables remain to be chosen independently in order to determine completely the state of the system. Thus, *Duhem's theorem* (Prigogine and Defay, 1954) states that *the equilibrium state of a closed system, for which the bulk composition is given, is completely determined by two independent variables.*

As previously stated, the two independent variables of interest for the purpose of this paper are temperature and pressure. Thus, by specifying a bulk composition, temperature, and pressure the state of a closed system is completely determined and, in general, will be divariant or polyvariant in the phase rule sense of variance or degrees of freedom. For a more complete discussion of the choice of the independent variables (both extensive and intensive) and their implications on the variance of the system see Prigogine and Defay (1954).

METHOD OF CALCULATION

Geometric interpretation.—Before beginning the detailed mathematical considerations requisite for the computation of equilibrium phase assemblages, it is convenient to illustrate the technique geometrically. One useful method of examining isothermal-isobaric phase equilibria is through the use of free energy-composition diagrams. Standard textbooks on thermodynamics, such as Darken and Gurry (1953), will, therefore, usually include discussions of simple binary examples in which isothermal-isobaric free energy-composition diagrams are discussed in relation to temperature-composition diagrams and to activity-composition diagrams. The same approach is useful in the present case, and free energy-composition diagrams are used below to illustrate our method of computating equilibrium phase assemblages.

Consider a binary system of components 1 and 2 in which the possible phases are B and A composed only of components 1 and 2, respectively, and C, a solution phase containing both components 1 and 2. Figure 1 is a series of free energy (G) versus composition (X) diagrams for this binary system showing the relations among the phases A, B, and C. The problem to be solved is the determination of the stable phase assemblage at some bulk composition, which will be represented by the composition *BC*.

In order to solve for the stable phase assemblage, a chemical potential line (μ_1-μ_2) is arbitrarily chosen with values of μ_1 and μ_2 which are sufficiently low (large negative quantities) so that all free energy points for pure phases and surfaces for solution phases are above the line μ_1-μ_2 (that is, they have more positive values than the line μ_1-μ_2). This initial

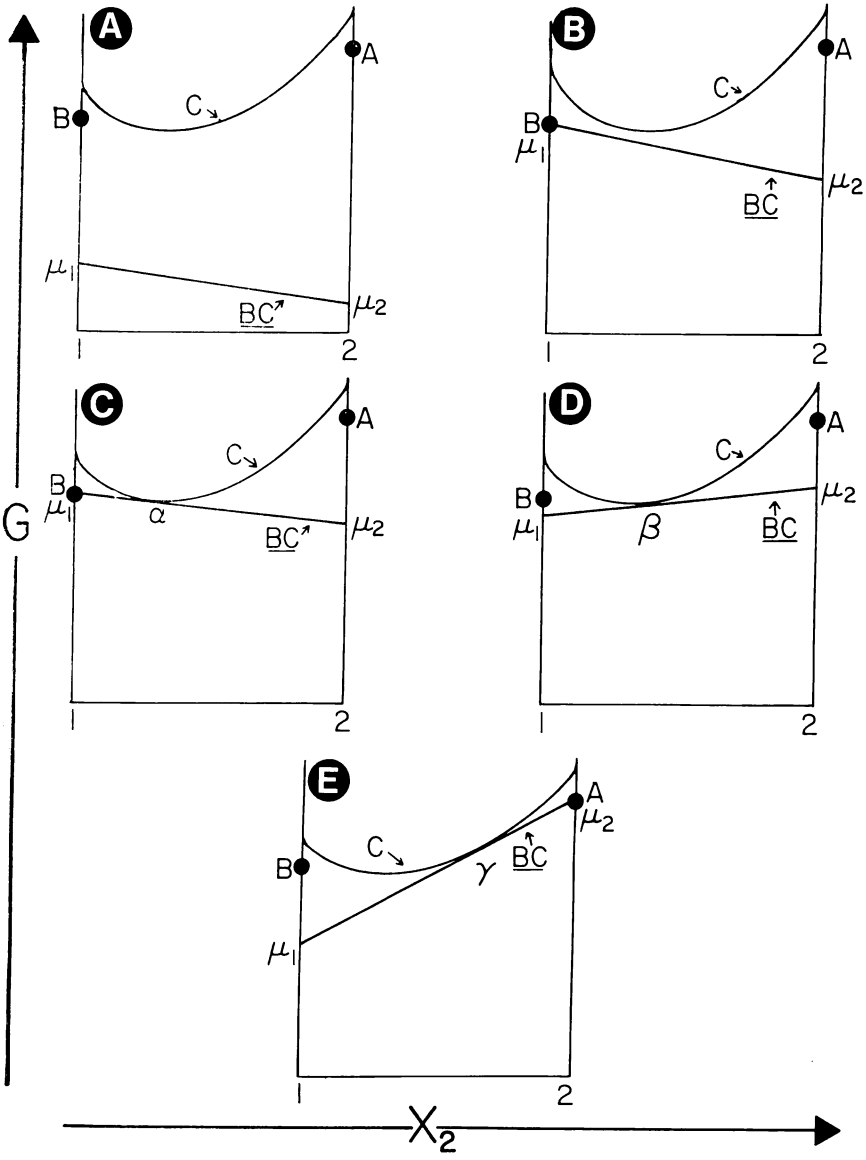

Fig. 1. Geometric representation of the computational method used in this paper. Diagrams for Gibbs free energy (G) versus composition (X) in the binary systems 1-2, containing pure phases A and B and solution phase C. The line μ_1-μ_2 is the chemical potential line being lifted to more positive values of G at the bulk composition point BC. Diagrams a to e are discussed at appropriate points in the text.

condition is illustrated in figure 1A. The chemical potential line is now "lifted" at the bulk composition *BC* such that the values of μ_1 and μ_2 become more positive. Because as yet there are no restrictions on the relative movement between μ_1 and μ_2, the line will be "lifted" parallel to its initial position. The line continues to be "lifted" until it intersects the point representing the free energy of phase B (fig. 1B). Because the chemical potential line cannot be above any free energy point or surface unless metastable equilibrium is desired, the line's continued upward movement is restricted and must now pivot on point B. Continued "lifting" of the line at point *BC* increases the chemical potential of component 2 while the chemical potential of component 1 remains constant. As illustrated in figure 1C, the chemical potential line finally intersects and becomes tangent to the free energy curve of phase C at a composition of C represented by point α. Because the chemical potential line is now restricted by the two phases B and C, it cannot be "lifted" upward at point *BC* and thus represents an equilibrium condition. However, in this stable assemblage of phases B and C (with a composition of α), the mass of phase B must be negative in order for the assemblage to have a bulk composition of *BC*. Therefore, phase B is removed as a restriction for continued upward movement of point *BC* on the chemical potential line. As the line continues to be "lifted" upward at point *BC*, it is now rotating on the free energy surface of phase C.

Figure 1D shows a position of the line after it has moved the tangent point with phase C's free energy surface from α to β. Continued increase in the free energy at point *BC* increases the chemical potential of component 2 and decreases the chemical potential of component 1 until the line intersects the free energy point for phase A (fig. 1E). This phase assemblage of A and C with a composition of γ again restricts the upward movement of point *BC* and represents an equilibrium assemblage. Because the masses required of phases A and C_γ to have the bulk composition *BC* are both positive, this assemblage answers the initial problem of finding the equilibrium phase assemblage for the bulk composition *BC*.

The approach illustrated above can be extended to multicomponent systems with the chemical potential line becoming a plane in three component space and a hyperplane in higher order component space. Although the chemical potential surface for systems with more than three components is an n-dimensional hyperplane, it will simply be termed the chemical potential plane in the discussions that follow. It is important to note that although we use the phrase chemical potential plane to describe the arbitrary free energy plane in discussing the computative method, we *do not* use the phrase in the strict thermodynamic sense.

Theoretical considerations.—Having demonstrated a conceptual and geometric framework by which an equilibrium assemblage might be computed, we will now examine the thermodynamic equations and relations that will allow us to compute the stable assemblage for the general case. The conceptual model is simple, as is the general case, and it is, therefore, hoped that the generalized notation and number of equations

that follow will not make the computation of equilibrium phase assemblages seem more difficult than it actually is.

In a system with n components the chemical potential plane or free energy plane at constant temperature and pressure can be expressed as

$$G_j = \sum_{i=1}^{n} N_{i,j}\mu_i \tag{1}$$

where G_j is the Gibbs free energy per mole of the jth composition; $N_{i,j}$ is the mole fraction of the ith component in the jth composition; and μ_i is the chemical potential of the ith component. We will reserve the subscript BC to represent the various properties of the bulk composition; for example, G_{BC} is the Gibbs free energy of the bulk composition.

The free energy of an m end member solution phase can be expressed by

$$G_j = \sum_{k=1}^{m} (X_{k,j}G^{\circ}_{k,j} + \alpha_{k,j}X_{k,j}\,RT\ln X_{k,j}) + G_{ex,j} \tag{2}$$

where G_j is the Gibbs free energy per component unit of the jth solution phase; $X_{k,j}$ is the mole fraction of the kth end member in the jth solution phase; $G^{\circ}_{k,j}$ is the Gibbs free energy per mole of the kth end member; $\alpha_{k,j}$ is the number of solution sites per formula unit of the kth end member of the jth solution phase; R is the gas constant; T is the absolute temperature; and $G_{ex,j}$ is the excess free energy function of the jth phase.

For ideal solutions $G_{ex,j}$ will, by definition, be equal to zero. In the derivations that follow, the excess free energy function will be carried in a general manner. In addition, a specific example, the regular symmetrical excess function (Thompson, 1967, p. 359), will be carried in the derivations. The regular symmetrical excess function for an m end member solution phase is defined by

$$G_{ex,j} = \sum_{k=1}^{m-1} X_{k,j} \sum_{t=k+1}^{m} X_{t,j}\,W_{kt} \tag{3}$$

where W_{kt} is the Margules parameter (Thompson, 1967) for the binary kt.

As previously stated the initial condition of the chemical potential plane will have values of μ_i chosen sufficiently low such that the free energies of all possible phases lie above the plane. However, as the chemical potential plane is "lifted" at the bulk composition point, the free energy of each phase is compared to the free energy of its compositionally equivalent point on the plane computed by using equation (1). For pure phases the computed value from equation (1) is simply compared to the tabulated free energy value for the phase at the specified temperature and pressure. For solution phases, where the free energy is

a function of composition, we need only compare the free energy values between equations (1) and (2) at compositions that have the same slope or partial derivatives on the two functions. This occurs because equation (1) must be tangent to equation (2), if equation (1) is in contact with equation (2).

In order to compute the compositions of the solution phases whose free energy relationship (eq 2) *would be tangent* to the initial chemical potential plane, we must introduce the relations between the chemical potential of the components (μ_i) and the chemical potential of the end members (k) of the jth solution phase ($\mu^*_{k,j}$). This relation can be expressed as

$$\mu^*_{k,j} = \sum_{i=1}^{n} \mu_i N_{i,k}. \tag{4}$$

The chemical potential plane can now be expressed for each solution phase as

$$G_j = \sum_{k=1}^{m} \mu^*_{k,j} X_{k,j} \tag{5}$$

where $X_{k,j}$ is again the mole fraction of the kth end member of the jth solution phase.

The partial derivatives of equations (5) and (2) with respect to the mole fraction of end member l with all other mole fractions of end members held constant except end member r, can be written as

$$\left(\frac{\partial G_j}{\partial X_l}\right)_{x_k, k \neq r} = \mu^*_{l,j} - \mu^*_{r,j} \tag{6}$$

and

$$\left(\frac{\partial G_j}{\partial X_l}\right)_{x_k, k \neq r} = G^\circ_{l,j} - G^\circ_{r,j} + \alpha_{l,j} RT \ln X_{l,j} - \alpha_{r,j} RT \ln X_{r,j} + (\alpha_{l,j} - \alpha_{r,j})\, RT + \left(\frac{\partial G_{ex,j}}{\partial X_l}\right)_{x_k, k \neq r} \tag{7}$$

where the derivative of the symmetrical regular excess function is

$$\left(\frac{\partial G_{ex,j}}{\partial X_l}\right)_{x_k, k \neq r} = \sum_{t=1, t \neq l}^{m} X_{t,j} W_{lt} - \sum_{t=1, t \neq r}^{m} X_{t,j} W_{rt} \quad . \tag{8}$$

Combining equations (6) and (7) we can write

$$\mu^*_{l,j} - \mu^*_{r,j} = G^\circ_{l,j} - G^\circ_{r,j} + \alpha_{l,j} RT \ln X_{l,j} - \alpha_{r,j} RT \ln X_{r,j} + (\alpha_{l,j} - \alpha_{r,j})\, RT + \left(\frac{\partial G_{ex,j}}{\partial X_l}\right)_{x_k, k \neq r}. \tag{9}$$

For an m member solution phase there will be $m - 1$ equations of the form of equation (9). In addition, we know that by definition

$$\sum_{k=1}^{m} X_{k,j} = 1. \tag{10}$$

Thus, for a given position of the chemical potential plane there are m equations ($m - 1$ equations of the form of (9) plus equation (10)) and m unknowns ($X_{k,j}$). If $G_{ex,j}$ is equal to zero, as in the case of an ideal solution, the m equations can be arranged into a set of simultaneous linear equations and can be solved for directly by matrix algebra. However, if $G_{ex,j}$ is not equal to zero, the equations for most excess functions will make the problem non-linear, and the $X_{k,j}$'s must be solved for by iteration. It will be shown below that this initial solution for the $X_{k,j}$'s for each phase need only be done once for each computation of an equilibrium phase assemblage.

Therefore, having established an initial arbitrary position of the chemical potential plane, we can compute, by using the set of equations represented by equations (9) and (10), the composition of the solution phases at the point on the free energy surface that would first contact the chemical potential plane if the plane is "lifted" parallel to its initial orientation. Thus, as long as the relative differences between the chemical potentials of the end members of a solution phase do not change, then the composition of the tangent point for the phase also does not change.

However, once movement of the chemical potential plane is restricted by its intersection of the free energy of one or more phases (that is, pivoting on points for pure phases and/or rotating tangential on the free energy surface of a solution phase), we must compute not only how the chemical potentials vary but also how the compositions of the tangent points of the solution phases change with an increase of the free energy at the bulk composition point BC. Because we are interested in how the chemical potentials of the components and the compositions of the solution phases vary with change in the free energy of the bulk composition, we can take the derivative of the function given in (1), with respect to the free energy of the bulk composition and express the derivative for the bulk composition point BC as

$$\sum_{i=1}^{n} N_{i,BC} \quad \frac{d\mu_i}{dG_{BC}} = 1. \tag{11}$$

A form of the Gibbs-Duhem equation at constant temperature and pressure can be written for each phase that is in contact with the chemical potential plane as

$$\sum_{i=1}^{n} N_{i,j} \frac{d\mu_i}{dG_{BC}} = 0. \tag{12}$$

By using equation (11) and an appropriate statement of equation (12) for each phase in contact with the chemical potential plane, we can solve for q + 1 values of $d\mu_i/dG_{BC}$ (where q equals the number of phases in contact with the plane). Thus, by assigning values to n–q–1 of the values of $d\mu_i/dG_{BC}$ (in actual calculations we normally assign zero), we can solve for the q + 1 values of $d\mu_i/dG_{BC}$.

For any given change in the free energy of the bulk composition (ΔG_{BC}) we can write a Taylor's expansion to compute the change in the chemical potential of the component as

$$\mu^n{}_i = \mu^o{}_i + \frac{d\mu_i}{dG_{BC}} \frac{\Delta G_{BC}}{1!} + \frac{d^2\mu_i}{dG^2{}_{BC}} \frac{\Delta G^2{}_{BC}}{2!} + \ldots . \tag{13}$$

where $\mu_i{}^n$ is the chemical potential of the ith component after the incremental change in G_{BC}, and $\mu^o{}_i$ is the chemical potential of the ith component at the previous position.

The new value of the free energy of the bulk composition is computed from

$$G^n{}_{BC} = G^o{}_{BC} + \Delta G_{BC}. \tag{14}$$

In practice we have found that equation (13) can be safely truncated after the first derivative term if the step size (ΔG_{BC}) is on the order of one calorie.

Having now moved the chemical potential plane to its new position, it is necessary to compute the new compositions of the solution phases that are or will be tangent to the plane. Instead of re-evaluating the set of functions represented by equations (9) and (10), which can be time consuming, especially if $G_{ex,j}$ is not zero, we solve for the compositional changes in an incremental manner.

The derivative of the function given in equation (9) with respect to G_{BC} can be expressed as

$$\begin{aligned} \frac{d\mu^*{}_{l,j}}{dG_{BC}} - \frac{du^*{}_{r,j}}{dG_{BC}} = {} & \frac{\alpha_{l,j}RT}{X_{l,j}} \frac{dX_{l,j}}{dG_{BC}} \\ & - \frac{\alpha_{r,j}RT}{X_{r,j}} \frac{dX_{r,j}}{dG_{BC}} \\ & + \frac{d\left(\frac{\partial G_{ex,j}}{\partial X_l}\right)_{x_k, k\neq r}}{dG_{BC}} \end{aligned} \tag{15}$$

where the regular symmetrical solution model is

$$\frac{d\left(\frac{\partial G_{ex,j}}{\partial X_l}\right)_{x_k, k\neq r}}{dG_{BC}} =$$

$$= \sum_{t=1, t\neq l}^{m} W_{lt} \frac{dX_{t,j}}{dG_{BC}} - \sum_{t=1, t\neq r}^{m} W_{rt} \frac{dX_{t,j}}{dG_{BC}} . \quad (16)$$

Also note that the derivative of the function given by equation (10) can be written as

$$\sum_{k=1}^{m} \frac{dX_{k,j}}{dG_{BC}} = 0. \quad (17)$$

As shown above, for each solution phase there will be $m - 1$ equations of the form of equation (15), and with the addition of equation (17), there will be m equations and m unknowns.

It can be seen by inspection that equations (15), (16), and (17) are linear functions of $dX_{k,j}/dG_{BC}$. Thus, $dX_{k,j}/dG_{BC}$ can be computed directly, and an iterative solution of equations (8), (9), and (10) can be avoided.

Having computed the change in composition with an incremental change in G_{BC}, we can compute the new solution compositions from a truncated Taylor's expansion similar to equation (13). This expansion can be expressed as

$$X^{n}_{k,j} = X^{o}_{k,j} + \frac{dX_{k,j}}{dG_{BC}} \Delta G_{BC} + \ldots . \quad (18)$$

where the superscripts n and o again refer to the new and old mole fractions respectively.

Equation (1) is now evaluated for each phase, and the free energies on the plane are compared to the tabulated free energies of pure phases and to the free energies that are computed for solution phases from equation (2). If the chemical potential plane has intersected an additional free energy point or surface, then the new phase will add an additional function like equation (12) and enable one more $d\mu_i/dG_{BC}$ to be computed. If no additional phase is encountered then the process, beginning with equation (11), is repeated.

If during the computational procedure when all n derivatives of the chemical potentials are being solved, the plane is not able to move upward at the point BC (that is, to a more positive value), then the plane is accepted as defining an equilibrium assemblage. The assemblage must have positive amounts of each phase in order for the assemblage to be the correct one for the bulk composition initially chosen. If any phase has a negative mass, then that phase is removed as a constraint on the continued upward movement of the plane by removing the appropriate statement of equation (12) for that phase, and the calculations are repeated again beginning with equation (11).

To compute the relative amount of each phase we need to write a mass balance equation for each component, which can be expressed as

$$\sum_{j=1}^{q} N_{i,j} Y_j = N_{i,BC} \tag{19}$$

where Y_j is the mole fraction of the jth phase in the assemblage; $N_{i,BC}$ is the mole fraction of the ith component of the bulk composition; and q is again the number of phases in contact with the chemical potential plane. There will be n such statements of equation (19) and q unknowns (Y_j's). If n equals q then the solution for the unknown values of Y_j is easily accomplished by matrix algebra. If, however, n is greater than q then a least squares regression of the n equations is done to determine the relative masses. The regression procedure is, of course, similar to that discussed by Bryan, Finger, and Chayes (1969) and by Wright and Doherty (1970). The regression is necessary because of small errors introduced into the compositions of the solution phases by the incremental procedure. If q is greater than n, the assemblage represents an invariant or univariant assemblage, and the relative masses cannot be computed.

Summary of computational method.—The procedures used in carrying out the calculation of an equilibrium phase assemblage for the general case can be summarized as follows:

1. Arbitrarily set initial position of chemical potential plane.
2. Solve for initial tangent points for all solution phases with equations (9) and (10).
3. Lift plane parallel to initial plane until first intersection with the free energy function of a phase.
4. Solve for $d\mu_i/dG_{BC}$ using equations (11) and (12).
5. Solve for $dX_{k,j}/dG_{BC}$ using equations (15) and (17).
6. Take increment of G_{BC} and solve for new values of μ_i, $X_{k,j}$, and G_{BC} with equations (13), (18), and (14), respectively.
7. Compute values of G_j for solution phases from equation (2) using new compositions of phases.
8. Compute free energy values on the plane for all phases considered by using equation (1).
9. Compare computed (equation (1)) free energy values on plane with the free energy of each phase to determine if plane has intersected free energy points or surfaces of remaining phases. If plane has intersected a new point or surface, place additional restriction on plane movement by a new equation (12) for that phase. If there is no intersection, return to procedure 4 above and repeat calculations.
10. Test assemblage with the set of equations represented by equation (19) to determine relative amounts of each phase. If amount of any phase is negative, remove the phase from restricting the plane by removing equation (12) for that phase. Return to 4 above and continue the calculation. If all phases have positive amounts, then calculation is finished and represents the equilibrium phase assemblage.

CONCLUSIONS

The differential equations derived above make it possible to predict equilibrium phase assemblages for multicomponent systems of considerable complexity in a reasonable calculation time. Although the method is incremental in nature, the equations at any given step in the process are linear, which makes the calculations amenable to rapid machine computation. A general computer program based on this approach has been written in Fortran. The computation time required for systems with up to 15 components is on the order of one minute on an IBM-370-155. With the thermodynamic data currently available, calculations can be carried out for a large number of multicomponent systems of geologic interest and will hopefully aid in the planning, interpretation, and evaluation of both experimental and field problems.

PART 2. APPLICATIONS

INTRODUCTION

Part 1 of this paper contains a summary of the thermodynamic principles, definitions, and relations needed for the calculation of equilibrium phase assemblages. In Part 2 we apply the principles to several analyzed rocks by calculating the equilibrium mineral assemblages under differing conditions and comparing them with the observed modes. The examples we have selected are intended to demonstrate two points: firstly, the method of computation; and secondly, that the existing thermodynamic data base is adequate, despite obvious deficiences, for making very useful calculations. Readers wishing to perform similar calculations can obtain a copy of the program listing by writing to the authors.

SOURCE OF DATA

The predicted appearance and predicted composition of a given mineral within a mineral assemblage is necessarily a function of the thermodynamic data used in the computations. Poor data lead to incorrect predictions.

Heat of formation, entropy, heat capacity, and volume for each solid phase considered in the calculations, which follow, were taken from Kelley (1960), Robie and Waldbaum (1968), Helgeson (1969), and Zen (1972) or were estimated directly from experimentally established equilibrium phase assemblages. Thermodynamic data for H_2O were taken from Burnham, Holloway, and Davis (1969). Data for CO_2 up to a pressure of 1400 bars were taken from Robie (1966) and for higher pressures were estimated by use of a corresponding state calculation (P. M. Orville, personal commun., 1973).

It is not the purpose of this paper to provide an accurate and internally consistent set of thermodynamic data. For this reason the data used were taken directly from the literature and are not repeated here. Such data are, of course, subject to change as newer refinements and better measurements become available. Several people (for example, Zen, 1972; Gordon, 1973; and Fisher and Haas, 1973) are working on various

aspects of accuracy, internal consistency, and quality of thermodynamic properties of minerals. As their work and that of others becomes available, the exactitude of the computed mineral assemblages can be continuously refined. Despite the present uncertainties in the thermodynamic data base, however, the calculated assemblages presented in this paper are in generally excellent agreement with the observed modes.

Three points concerning our use of data and computations must be mentioned. Firstly, Zen (1972) pointed out an inconsistency in the Gibbs free energy and heats of formation of various aluminous minerals. The source of the error has not yet been identified, so we arbitrarily adjusted the data of all aluminum compounds to be consistent with the heat of formation of corundum. Fortunately this decision does not affect the calculations presented below because an equilibrium phase assemblage is determined on a *relative* free energy basis. Secondly, in carrying out computations of Gibbs free energy for solid phases at elevated temperatures and pressures, we assumed that the volume of the solid phase remained constant. Because relative volume changes of all solid phases are approximately the same, the assumption of constancy of volume does not materially influence Gibbs free energy at pressures below 10 kb. Our third and final assumption concerned phases in which solid solutions are important. We have listed in table 1 all the names and compositions of the stoichiometric phases considered in this study. Included in the list are the solid solution phases together with the compositions of the end-members that we assume can be used to describe the solutions. For the purposes of our computations, we have assumed that both the solid and the fluid solution phases can be approximated by *ideal mixing* of the end-members. This assumption leads to minor difficulties in some of the predicted equilibrium assemblages. The difficulties are discussed below.

We stress that the calculations presented are intended as *examples* of the application of the method derived in part 1. Indirectly the calculations provide a general test of the thermodynamic data, but they cannot be accepted as definitive. Many changes, such as new data, refinements in computation, and better chemical analyses will allow more accurate prediction of phase assemblages in the future.

EXAMPLES OF COMPUTATIONS

To test both computational procedures and the general quality of the thermodynamic data base, we chose four metamorphic and three igneous rocks for which modes, chemical analyses, and some compositional data for the individual minerals are available. In choosing the temperatures and pressures for each calculation, we have not always selected the most geologically reasonable temperature and pressure of formation of each rock but have instead selected temperatures and pressures that are in or near the divariant field for each mode. The computed assemblages nevertheless match the modes rather closely, suggesting that bulk composition exerts a more important control on mineral assemblages than is commonly thought.

Igneous rocks.—Two of the most frequently analyzed igneous rocks are the granite G-1 and the diabase W-1. As a result, their compositions are known more precisely than most other rocks. The modes of G-1 and W-1 are also well known, having been determined by point count and statistical analysis by Chayes (1951). The compositions of G-1 and W-1 (Schlecht and Stevens, 1951) are shown in table 2, where the oxide components have been recomputed to 100 percent for the 12 components considered in our calculations.

Comparison of the observed mode (Chayes, 1951) of G-1 and our computed equilibrium assemblage for 600°C (873.15°K) and 2000 bars is illustrated in table 3. The pressure in this example, as with all other examples, is the total pressure on the system. The stable phases and the predicted masses of phases are in pleasingly close agreement with the observed mineralogy. Although Chayes' mode is in volume percent and our predicted assemblage is in weight percent, the densities of the minerals present are sufficiently close so that errors of comparison are small. The

TABLE 1

Composition of phases considered in the example calculations of equilibrium phase assemblges. Listed under the solution phases are the end members considered for the calculations

Oxides	
Quartz	SiO_2
Ferrous oxide	FeO
Periclase	MgO
Corundum	Al_2O_3
Soda	Na_2O
Lime	CaO
Rutile	TiO_2
Potash	K_2O
Water, steam	H_2O
Hematite	Fe_2O_3
Phosphorus pentoxide	P_2O_5
Carbon dioxide	CO_2
Non-silicates	
Ilmenite	$FeTiO_3$
Spinel	$MgAl_2O_4$
Magnetite	Fe_3O_4
Perovskite	$CaTiO_3$
Gibbsite	$Al(OH)_3$
Portlandite	$Ca(OH)_2$
Brucite	$Mg(OH)_2$
Anatase	TiO_2
Diaspore	$AlO(OH)$
Magnesite	$MgCO_3$
Dolomite	$CaMg(CO_3)_2$
Calcite	$CaCO_3$
Apatite	$Ca_5(PO_4)_3OH$
Whitlockite	$Ca_3(PO_4)_2$
Chain silicates	
Diopside	$CaMgSi_2O_6$
Hedenbergite	$CaFeSi_2O_6$
Enstatite	$MgSiO_3$
Ferrosilite	$FeSiO_3$
Jadeite	$NaAlSi_2O_6$
Ca-Al pyroxene	$CaAl_2SiO_6$
Wollastonite	$CaSiO_3$
Tremolite	$Ca_2Mg_5Si_8O_{22}(OH)_2$
Actinolite	$Ca_2Fe_5Si_8O_{22}(OH)_2$
Framework silicates	
K-feldspar (High sanidine)	$KAlSi_3O_8$
Anorthite	$CaAl_2Si_2O_8$
High-Albite	$NaAlSi_3O_8$
Low-Albite	$NaAlSi_3O_8$
Nepheline	$NaAlSiO_4$
Ortho- and ring-silicates	
Fayalite	Fe_2SiO_4
Forsterite	Mg_2SiO_4
Grossular	$Ca_3Al_2Si_3O_{12}$
Almandine	$Fe_3Al_2Si_3O_{12}$
Pyrope	$Mg_3Al_2Si_3O_{12}$
Sillimanite	Al_2SiO_5
Andalusite	Al_2SiO_5
Kyanite	Al_2SiO_5
Mg-Cordierite	$Mg_2Al_4Si_5O_{18}$
Fe-Cordierite	$Fe_2Al_4Si_5O_{18}$
Akermanite	$Ca_2MgSi_2O_7$
Monticellite	$CaMgSiO_4$
Merwinite	$Ca_3MgSi_2O_8$
Larnite	Ca_2SiO_4
Ca-Olivine	Ca_2SiO_4

predicted mass of K-feldspar shows the largest departure from the observed assemblage. This occurs because the calculated K-feldspar was considered to be a pure potassium compound without any sodium present in solid solution. The necessary refinement allowing sodium substitution could now be incorporated into the data base and computation. It would cause the predicted mass of K-feldspar to rise, that of plagioclase to fall, and the composition of the predicted plagioclase to become more anorthite-rich, but still to remain in the observed composition range. Individual users of this program must decide whether such refinements are necessary for the problems they are considering. Our calculations predict whitlockite to be stable over apatite for the conditions selected for G-1. It is not clear whether the thermodynamic data for whitlockite and/or apatite are in error, or whether the substitution of fluorine in apatite, a refinement not considered, would stabilize apatite over whitlockite.

Table 4 lists the mode (Chayes, 1951) and the predicted assemblage for W-1 at 700°C (973.15°K) and 1000 bars. In this example we have attempted to predict the composition of a complicated pyroxene using the

3 · 2 Mullite	$3Al_2O_3 \cdot 2SiO_2$
Gehlenite	$Ca_2Al_2SiO_7$
Zoisite	$Ca_2Al_3Si_3O_{12}(OH)$
Sheet silicates	
Muscovite	$KAl_3Si_3O_{10}(OH)_2$
Paragonite	$NaAl_3Si_3O_{10}(OH)_2$
Phlogopite	$KMg_3AlSi_3O_{10}(OH)_2$
Annite	$KFe_3AlSi_3O_{10}(OH)_2$
Margarite	$CaAl_4Si_2O_{10}(OH)_2$
Pyrophyllite	$Al_2Si_4O_{10}(OH)_2$
Talc	$Mg_3Si_4O_{10}(OH)_2$
Fe-Chlorite	$Fe_5Al_2Si_3O_{10}(OH)_8$
Clinochlore	$Mg_5Al_2Si_3O_{10}(OH)_8$
Kaolinite	$Al_2Si_2O_5(OH)_4$
Illite	$K_{0.6}Mg_{0.25}Al_{2.3}Si_{3.5}O_{10}(OH)_2$
Na-montmorillonite	$Na_{0.33}Al_{2.33}Si_{3.67}O_{10}(OH)_2$
Ca-montmorillonite	$Ca_{0.167}Al_{2.33}Si_{3.67}O_{10}(OH)_2$
K-montmorillonite	$K_{0.33}Al_{2.33}Si_{3.67}O_{10}(OH)_2$
Mg-montmorillonite	$Mg_{0.167}Al_{2.33}Si_{3.67}O_{10}(OH)_2$
Prehnite	$Ca_2Al_2Si_3O_{10}(OH)_2$
Chrysolite	$Mg_3Si_2O_5(OH)_4$
Solution phases	
Olivine	
Fayalite	Fe_2SiO_4
Forsterite	Mg_2SiO_4
Plagioclase	
Anorthite	$CaAl_2Si_2O_8$
Albite	$NaAlSi_3O_8$
Garnet	
Grossular	$Ca_3Al_2Si_3O_{12}$
Almandine	$Fe_3Al_2Si_3O_{12}$
Pyrope	$Mg_3Al_2Si_3O_{12}$
Tremolite-actinolite	
Tremolite	$Ca_2Mg_5Si_8O_{22}(OH)_2$
Actinolite	$Ca_2Fe_5Si_8O_{22}(OH)_2$
Cordierite	
Mg-cordierite	$Mg_2Al_4Si_5O_{18}$
Fe-cordierite	$Fe_2Al_4Si_5O_{18}$
Chlorite	
Clinochlore	$Mg_5Al_2Si_3O_{10}(OH)_8$
Fe-chlorite	$Fe_5Al_2Si_3O_{10}(OH)_8$
Montmorillonite	
Na-montmorillonite	$Na_{0.33}Al_{2.33}Si_{3.67}O_{10}(OH)_2$
Ca-montmorillonite	$Ca_{0.167}Al_{2.33}Si_{3.67}O_{10}(OH)_2$
K-montmorillonite	$K_{0.33}Al_{2.33}Si_{3.67}O_{10}(OH)_2$
Mg-montmorillonite	$Mg_{0.167}Al_{2.33}Si_{3.67}O_{10}(OH)_2$
Fluid phase	
Water	H_2O
Carbon Dioxide	CO_2
Biotite	
Phlogopite	$KMg_3AlSi_3O_{10}(OH)_2$
Annite	$KFe_3AlSi_3O_{10}(OH)_2$
Pyroxene	
Diopside	$CaMgSi_2O_6$
Hedenbergite	$CaFeSi_2O_6$
Enstatite	$Mg_2Si_2O_6$
Ferrosilite	$Fe_2Si_2O_6$
"Perovskite"*	$Ca_2Ti_2O_6$
Jadeite	$NaAlSi_2O_6$
Ca-Al pyroxene	$CaAl_2SiO_6$

* Although perovskite is not a pyroxene, its composition was used as a pyroxene end member to allow some titanium to enter the predicted pyroxene composition.

TABLE 2

Chemical analyses, in weight percent, of rocks used in the calculations. The analyses are recomputed to 100 percent for the 12 oxides considered

	Igneous rocks			Metamorphic rocks				
	G-1 Schlecht and Stevens (1951)	W-1 Schlecht and Stevens (1951)	12004 Brett and others (1971)	MF626 Frey (personal commun., 1973)	MF702 Frey (personal commun., 1973)	MF886 Frey (personal communi., 1973)	Ch-1 Chinner (1960)	"Average" Shale Clarke (1924)
SiO_2	72.37	52.43	45.26	58.58	60.20	44.78	43.36	59.81
$AlO_{1.5}$	14.32	15.11	8.37	10.24	28.64	18.42	32.65	15.85
FeO	1.02	8.81	21.47	8.26	0.98	3.92	6.64	2.52
$FeO_{1.5}$	0.95	1.62	—	0.03	0.76	1.01	0.48	4.13
MgO	0.40	6.59	12.70	3.48	0.24	2.82	3.16	2.51
CaO	1.40	10.98	9.17	7.46	0.03	9.76	1.01	3.20
$NaO_{0.5}$	3.31	2.07	0.20	0.23	0.61	1.41	1.54	1.34
$KO_{0.5}$	5.42	0.67	—	0.89	1.64	3.42	6.10	3.33
TiO_2	0.26	1.07	2.82	0.49	1.23	0.70	1.41	0.67
$PO_{2.5}$	0.10	0.20	—	0.09	0.04	0.12	0.01	0.17
$HO_{0.5}$	0.36	0.10	—	4.08	5.62	2.87	3.29	3.77
CO_2	0.08	—	—	6.17	0.01	10.77	—	2.70

solid solution end-members listed in table 1. Although the thermodynamic data, the assumption of ideal solution behaviour, and, perhaps, the choice of end-members do not warrant placing great reliance on the calculation, it is nevertheless interesting that the predicted pyroxene composition is reasonable for a diabase. It is also encouraging that the predicted assemblage agrees so well with the mode. However, the alumino-silicate appearing in the predicted assemblage is unreasonable and indicates that the pyroxene composition should probably be more aluminous and less calcic. Presently available data do not permit us to refine this computation. If it were possible to do so, some of the quartz and the alumino-silicate would probably go into both the pyroxene and the plagioclase. As a consequence, some of the calcium from the pyroxene would make the plagioclase more anorthite-rich and bring the predicted masses even closer to the observed.

TABLE 3

Comparison of observed mode (Chayes, 1951) of G-1 and computed equilibrium assemblage at 600°C (873.15°K) and 2000 bars

Mode; volume percent		Equilibrium assemblage; weight percent	
Quartz	27.5	Quartz	29.6
K-feldspar	35.4	K-feldspar	28.6
Plagioclase An_{10-30}	31.4	Plagioclase An_{18}	34.5
Biotite	3.2	Biotite $Annite_{16}$	2.79
Muscovite	1.3	Muscovite	2.53
Opaques	0.8	Magnetite	1.38
Accessories	0.4	Rutile	0.26
		Whitlockite	0.19
		Fluid Phase ($X_{H_2O} = 0.89$, $X_{CO_2} = 0.11$)	0.22

TABLE 4

Comparison of observed mode (Chayes, 1951) of W-1 and computed equilibrium assemblage at 700°C (973.15°K) and 1000 bars

Mode; weight percent		Equilibrium assemblage; weight percent	
Pyroxene	45.0	Pyroxene*	43.0
Plagioclase An_{50-70}	45.0	Plagioclase An_{50}	40.2
K-feldspar	3.0	K-feldspar	3.3
Quartz	1.8	Quartz	5.2
Biotite	1.8	Biotite $Annite_{47}$	1.1
Opaques	3.3	Magnetite	2.4
Accessories	0.2	Rutile	0.4
		Apatite	0.4
		Al_2SiO_5	3.15

* Predicted pyroxene composition: $Ca_{0.52}Fe_{0.56}Mg_{0.85}Na_{0.01}Ti_{0.04}Al_{0.06}Si_{1.93}O_6$.

TABLE 5

Comparison of observed mode (Brett and others, 1971) of Apollo 12 rock 12004 and computed equilibrium assemblage at 1000°C (1273.15°K) and 1 bar

Mode; volume percent		Equilibrium assemblage; weight percent	
Pyroxene	57.2	Pyroxene*	61.00
Plagioclase An_{91}	19.7	Plagioclase $An_{93.5}$	21.00
Olivine Fa_{23-35}	15.0	Olivine Fa_{16}	13.00
Opaques (ilmenite and ülvospinel)	4.9	Ilmenite	5.00
Other	3.2		

* Predicted pyroxene composition: $Ca_{0.35}Mg_{0.88}Fe_{0.73}Na_{0.006}Al_{0.066}Ti_{0.011}Si_{1.96}O_6$.

Our final example of an igneous rock is a chemically simpler one than either G-1 or W-1. Rock 12004, collected on Apollo 12 mission to the Moon, is a mare basalt for which several chemical analyses are available. The average composition listed in table 2 and the mode listed in table 5 are from Brett and others (1971). Our predicted mineral assemblage for 1000°C (1273.15°K) and 1 bar (table 5) is in excellent agreement with the mode both in respect to the predicted stable phases and to their respective masses. As in the calculation for W-1, we have employed the possibly overly complicated pyroxene model. Although the actual pyroxene compositions were not measured by Brett and others, analyses of pyroxenes in other, similar, Apollo 12 rocks (that is, Bence, Papike, and Lindsley, 1971) are available. These are all, on the average, subcalcic augites, and even the sodium, aluminum, and titanium contents in our predicted pyroxenes are in general agreement with the observations.

Metamorphic rocks.—Metamorphic rocks, in general, display a greater diversity of compositions, temperatures, and pressures of formation than do igneous rocks. As a consequence, they have been more difficult to deal with by conventional normative calculations such as the CIPW system (Cross and others, 1903). Our program provides a convenient way to circumvent previous difficulties; to demonstrate the potential of the method we have selected three low grade and one high grade metamorphic rocks.

For low temperature metamorphic assemblages we have used three lower greenschist facies rocks from the Glaris Alps studied by Frey (personal commun., 1973). Analyses of the three rocks MF626, MF702, and MF886 are listed in table 2, and their modes, determined by X-ray diffraction as well as petrographic analyses, are presented with their computed assemblages in tables 6, 7, and 8.

The calculation for MF886 given in table 6 is for 340°C (613.15°K) and 3000 bars. The predicted mineral assemblage agrees closely with Frey's observations, but the predicted masses of phases differ slightly from the observed. The reason for the mass differences lies, probably, in

the temperature selected for computation. At lower temperatures or higher pressures, plagioclase, some of the chlorite, and the fluid phase will react to form additional dolomite, paragonite, quartz, and a more water-rich fluid phase. It is interesting to observe the high CO_2 content predicted for the composition of the metamorphic fluid in this calculation.

The assemblage calculated for sample MF626 (table 7) is for 300°C (573.15°K) and 2000 bars. The predicted mineral assemblage matches the observed mineralogy, except for the predicted kaolinite, but, again, the predicted masses of phases differ slightly from those observed. The mass differences in this example as well as the appearance of kaolinite can be reduced by calculating assemblages at higher temperatures and/or lower pressure. This occurs because some of the kaolinite, talc, and dolomite react to form additional chlorite, calcite, and quartz.

Table 8 compares the mode and predicted assemblage at 300°C (573.15°K) and 1000 bars for sample MF702. As with the previous two examples the observed mineralogy agrees with the computed assemblage, but disagreement occurs between the predicted and observed masses of phases. In addition, our computed assemblage contains kaolinite, a phase not observed by Frey. The discrepancies could probably be resolved if a higher temperature and/or lower pressure were selected. Under these circumstances the reaction of kaolinite and quartz to produce pyrophyllite and a more water-rich fluid phase would probably occur. Kaolinite would no longer be in the predicted assemblage, and the mass of pyrophyllite

TABLE 6

Comparison of observed mode (Frey, personal commun., 1973) of sample MF886 and computed equilibrium assemblage at 340°C (613.15°K) and 3000 bars

Mode; weight percent		Equilibrium assemblage; weight percent	
Quartz	28	Quartz	21.5
Muscovite	30	Muscovite	28.9
Muscovite/ paragonite*	5-10		
Paragonite	5-10	Paragonite	14.4
Calcite	10	Calcite	10.3
Dolomite	14	Dolomite	12.5
Chlorite	5	Chlorite ($X_{Fe} = 0.96$, $X_{Mg} = 0.04$)	7.9
		Plagioclase An_3	2.13
		Apatite	0.28
		Rutile	0.70
		Magnetite	0.25
		Hematite	0.83
		Fluid Phase ($X_{H_2O} = 0.6$, $X_{CO_2} = 0.4$)	0.33

* Mixed layer phase of muscovite and paragonite (Frey, 1969).

TABLE 7

Comparison of observed mode (Frey, personal commun., 1973) of sample MF626 and computed equilibrium assemblage at 300°C (573.15°K) and 2000 bars

Mode; weight percent		Equilibrium assemblage; weight percent	
Quartz	47	Quartz	42.9
Muscovite-illite	10-15	Muscovite	7.57
Paragonite/muscovite	+?		
Paragonite	+?	Paragonite	2.82
Chlorite	25	Chlorite ($X_{Fe} = 0.67$, $X_{Mg} = 0.33$)	22.8
Calcite	14	Calcite	11.0
Dolomite	1	Dolomite	2.67
		Kaolinite	6.80
		Talc	1.77
		Apatite	0.21
		Sphene	1.20
		Hematite	0.03
		Fluid phase ($X_{H_2O} = 0.92$, $X_{CO_2} = 0.08$)	0.11

TABLE 8

Comparison of observed mode (Frey, personal commun., 1973) of sample MF702 and computed equilibrium assemblage at 300°C (573.15°K) and 1000 bars

Mode; weight percent		Equilibrium assemblage; weight percent	
Quartz	14	Quartz	8.30
Muscovite-illite	10	Muscovite	13.83
Paragonite/muscovite*	<5	Paragonite	7.56
Chlorite	<5	Chlorite ($X_{Fe} = 0.69$, $X_{Mg} = 0.31$)	2.63
Pyrophyllite	70	Pyrophyllite	53.7
		Kaolinite	11.9
		Rutile	1.23
		Hematite	0.76
		Whitlockite	0.056
		P_2O_5	0.015
		Fluid phase ($X_{H_2O} = 0.85$, $X_{CO_2} = 0.15$)	0.022

* Mixed layer phase of muscovite and paragonite (Frey, 1969).

would more closely match that of the mode. However, the mass of quartz would then be more than 10 percent below the observed value. Changing the physical conditions selected for the computed assemblage will not, therefore, bring close concordance between observed and predicted mineralogy. We suggest that in this case our calculations could point to an error in either the chemical analysis or the reported mode. For example, the analysis might be too low in silica or some of the pyrophyllite reported in the mode may actually be kaolinite. The appearance of P_2O_5 in our predicted assemblage points to another problem. Either there is an error in the calcium or phosphorus analyses, or other phosphate phases are present and should be considered in the calculations.

For an example of a high grade metamorphic rock we have selected a pelitic gneiss (Ch-1) studied by Chinner (1960). The chemical composition of this rock is given in column 7 of table 2, while the observed mode and equilibrium assemblage computed for 726.85°C (1000°K) and 1000 bars are presented in table 9. The observed and predicted mineral assemblages are in good agreement. The prediction of andalusite as the stable phase reflects the pressure selected for computation. The mass discrepancies between observed and predicted assemblages point out one limitation of using an ideal solid solution of phlogopite and annite for the biotite solid solution. If thermodynamic data were available, or could be estimated, for the eastonite and siderophyllite end-members of the biotite solid solution, these components could be computed into the biotite composition, using the K-feldspar, some of the aluminum silicate, and water in the process. Both the predicted masses and the mineral compositions would thereby match the observed more closely.

Changing assemblages with changing P-T conditions.—As a final example of computation we have selected a single rock composition and computed the mineral assemblages under four different conditions. This kind of computation allows one to provide rapid answers to questions

TABLE 9

Comparison of observed mode (Chinner, 1960) of sample Ch-1 and computed equilibrium assemblage at 726.85°C (1000°K) and 1000 bars

Mode; volume percent		Equilibrium assemblage; weight percent	
Muscovite	26.3	Muscovite	25.5
Biotite $(X_{Fe})/(X_{Fe} + X_{Mg}) = 0.54$	33.9	Biotite Annite$_{53.7}$	26.3
Kyanite + sillimanite	21.8	Al_2SiO_5 (andalusite)	24.4
Plagioclase An_{10-20}	16.4	Plagioclase An_{20}	17.8
Magnetite	0.8	Magnetite	0.7
Ilmenite	0.8	Rutile	1.42
Apatite	tr	Apatite	0.004
		K-feldspar	2.75
		H_2O	1.2

such as, what mineral assemblages would an "average" shale develop as it is metamorphosed along a given temperature-pressure path, or, given an analysis performed by remote control on the surface of another planet, what mineral assemblages might be present under any postulated conditions of formation?

In column 8 of table 2 we have listed the composition of "average" shale given by Clarke (1924), and in table 10 we have computed the equilibrium assemblages under four different sets of physical conditions.

The phases predicted for 25°C and a pressure of 1 bar (table 10, column 1) are very similar to those observed in many sediments and many shales. This fact may seem surprising for a rock composed largely of detrital grains, and that suggests detrital sediments do start to approach equilibrium with their environment. Some predictions deserve comment. For example, low albite is predicted to be stable with respect to paragonite and a sodium-rich montmorillonite from the data used in our calculations. We cannot differentiate between an error in the data selected and the possibility that low albite is stable. Because low albite is known to form under sedimentary-diagenetic conditions both possibilities have equal likelihoods. Another prediction from our computations should be treated with caution—the prediction of the fluid composition. Water and carbon dioxide have an immiscibility gap at 25°C and 1 bar, but we have nevertheless used an ideal solution model for the solution phase. The composition computed for the fluid falls in a one phase region and, surprisingly, coincides with the composition of water in equilibrium with the present day atmosphere.

Many fine-grained sediments contain amorphous silica and as a consequence many natural aqueous solutions at low temperatures are probably supersaturated with respect to quartz. We therefore repeated the "average" shale computation at 25°C and 1 bar but suppressed quartz. This was effected by removing quartz from the list of possible phases and replacing it by amorphous silica. The results of this computation (table 10, column 2) show that the mineral assemblage is not greatly changed. Illite, talc, and calcite form at the expense of silica, muscovite, dolomite, and magnesian chlorite.

When the temperature is raised to 300°C and the pressure to 1000 bars, but the system is kept closed to losses of volatiles, the assemblage listed is column 3 of table 10 as predicted. The low temperature albite has now reacted to form paragonite and an albite-rich plagioclase (An_4). The amount of calcite and talc have increased at the expense of dolomite and some of the magnesian chlorite, while the amount of fluid phase has increased, and it has become considerably richer in CO_2.

Maintaining pressure at 1000 bars but increasing temperature to 500°C produces many changes in the predicted mineral assemblage (table 10, column 4). Plagioclase increases in amount and becomes more anorthitic (An_{45}). The amount of muscovite decreases as biotite appears in the assemblage and an aluminum-rich, augitic pyroxene forms. All the CO_2 now resides in the fluid phase because calcite has been eliminated

TABLE 10

Predicted equilibrium assemblages at various temperatures and pressures for "average" shale (see table 2). Quantity of each phase is given in weight percent

Phase	(1) 25°C, 1 bar	(2) 25°C, 1 bar (Quartz suppressed)	(3) 300°C, 1000 bars	(4) 500°C, 1000 bars	(5) 700°C, 1000 bars
Quartz	33.06	—	33.05	31.52	26.16
Amorphous silica	—	26.92	—	—	—
Chlorite	7.77 ($X_{Fe} = 0.58$)	5.11 ($X_{Fe} = 0.97$)	6.73 ($X_{Fe} = 0.69$)	—	—
Talc	2.60	4.18	5.91	—	—
Low albite	11.35	11.35	—	—	—
Plagioclase	—	—	7.34 (An_4)	19.34 (An_{45})	17.43 (An_{40})
High-sanidine	—	—	—	—	19.67
Muscovite	28.16	8.50	28.16	23.23	—
Illite	—	31.57	—	—	—
Paragonite	—	—	6.31	—	—
Kaolinite	4.07	—	—	—	—
Biotite	—	—	—	5.38 ($Annite_{15}$)	—
Calcite	2.77	4.52	4.34	—	—
Dolomite	3.11	1.43	—	—	—
Pyroxene	—	—	—	7.57*	12.64**
Andalusite	—	—	—	0.80	11.09
Anatase	—	0.66	—	0.58	0.51
Sphene	1.63	—	1.63	—	—
Apatite	0.41	0.41	0.41	—	—
Whitlockite	—	—	—	0.38	0.38
Hematite	4.13	4.13	4.13	1.10	0.83
Magnetite	—	—	—	4.39	4.77
Fluid phase	0.94 ($X_{H_2O} = 0.9997$, $X_{CO_2} = 10^{-3.54}$)	1.21 ($X_{H_2O} = 0.994$, $X_{CO_2} = 10^{-2.22}$)	1.98 ($X_{H_2O} = 0.88$, $X_{CO_2} = 0.12$)	5.20 ($X_{H_2O} = 0.82$, $X_{CO_2} = 0.18$)	6.47 ($X_{H_2O} = 0.87$, $X_{CO_2} = 0.13$)

* Predicted pyroxene composition: $Ca_{0.58}Fe_{0.27}Mg_{0.02}Al_{0.20}Na_{0.08}Ti_{0.03}Si_{1.91}O_6$.
** Predicted pyroxene composition: $Ca_{0.47}Fe_{0.25}Mg_{1.07}Al_{0.22}Na_{0.07}Ti_{0.03}Si_{1.89}O_6$.

from the assemblage. Raising the temperature to 700°C and 1000 bars (table 10, column 5) results in the appearance of an anhydrous mineral assemblage that is predominantly quartz, plagioclase, K-feldspar, pyroxene, and andalusite.

Although "metamorphism" of shale in a closed system such as we have presented in table 10 produces mineral assemblages that appear to be, in general, similar to those one might expect, the process cannot be considered entirely reasonable on geological grounds, because a closed system is geologically unreasonable. The mass of fluid phase predicted, especially in the 500° and 700°C calculations, would occupy a large volume at 1000 bars. In nature they probably escape from the system during metamorphism. Because carbonate minerals react to leave the predicted assemblage before all the hydrous minerals do, more CO_2 would escape, relatively, than H_2O, and as a consequence the chemical potential of H_2O under real conditions of metamorphism would be higher than in the closed system used for our computations. Hydrous minerals would therefore persist to higher temperatures than predicted in the closed system. Also, the calculation we have performed is geologically unreasonable in two other respects. Reduction of ferric iron cannot occur in the closed system as calculated, and if the system were open, alkalies would probably be added to the system in which case they would react with the andalusite to form additional feldspars.

Although it is not possible to use our program for open systems *sensu stricto*, calculations can be made to approximate systems that are open to the fluid phase by isothermally-isobarically adding or subtracting fluid phase of the appropriate composition in an incremental manner. There are probably many applications that can be reduced to asking the question for a given bulk composition, temperature, and pressure: What should the equilibrium assemblage be?

DISCUSSION AND CONCLUSIONS

From the examples of calculated equilibrium mineral assemblages presented, it is apparent that the method can be used to help solve some of the problems of multicomponent rocks. We repeat, however, that care must be exercised in interpreting the computed results. Some of the questions which should be raised for each computation are:

1. Are there errors in the thermodynamic data that could affect the assemblages predicted by the calculation?
2. How does the solution phase model (that is, the mixing assumptions, the mixing parameters, the end-members used, et cetera) affect the calculated results?
3. Have any phases been omitted from consideration, either intentionally or owing to lack of thermodynamic data, that should be in the stable assemblage?
4. Are there errors in the chemical analysis and/or modes of the rock that could account for discrepancies between observed and predicted assemblages?

Assuming the questions can be answered satisfactorily, the calculation of equilibrium mineral assemblages should ultimately prove useful in a variety of circumstances. Differences between modes and predicted mineral assemblages might point to possible kinetic and reaction rate problems. Experimental petrologists might make use of the calculations in planning and interpreting their experiments. One could, for example, compute P-T diagrams for complicated rock compositions once the thermodynamic data have been tested adequately. As demonstrated in several of the examples (that is, MF886 and MF626) complicated multicomponent reactions can be observed, and their effects on the assemblages assessed. Once identified, they could be tested by field observations or experiments. Two vital and very important tests can be performed: testing of new thermodynamic data and testing modes and chemical analyses by comparing them with computed assemblages. Indeed, we suggest that all rock analyses should be tested by comparing computed equilibrium assemblages with the mode.

Additional refinements can be or are being made to the program. These include the addition of the asymmetrical solution model (Thompson, 1967), the ability to compute assemblages directly as a function of temperature and pressure, and being able to specify variables other than temperature and pressure (that is, constant volume, entropy, et cetera). Melt equilibria could also be added to the program, thereby opening a wider range of problems to analysis. For example, by adding the Gibbs free energy relations of silicate melts, one could make calculations to test ideas such as partial melting and the solubility of minerals in melts.

Through the use of equilibrium assemblage calculations we suggest that petrologists and geochemists will be able to solve, or at least better understand, some of the problems associated with the processes of rock formation.

ACKNOWLEDGMENTS

We are indebted to Harold C. Helgeson, Philip M. Orville, Martin Frey, and Louis Fernandez for their encouragement, helpful suggestions, and constructive criticism during various stages of the development of this paper. We are particularly indebted to Martin Frey for allowing us to have access to his valuable results on low grade metamorphic rocks from the Alps prior to formal publication of his data. We thank Priestley Toulmin for reviewing the paper and offering many helpful suggestions.

The work reported here was supported in part by research funds received from NASA, grant NGR 07-004-157.

REFERENCES

Bence, A. E., Papike, J. J., and Lindsley, D. H., 1971, Crystallization histories of clinopyroxenes in two porphyritic rocks from Ocean Procellarum: M.I.T. Press, Second Lunar Sci. Conf. Proc., v. 1, p. 559-574.

Brett, P. R., Butler, P., Jr., Meyer, C., Jr., Reid, A. C., Takeda, H., and Williams, R., 1971, Apollo 12 igneous rocks 12004, 12008, 12009 and 12022: A mineralogical and petrological study: M.I.T. Press, Second Lunar Sci. Conf. Proc., v. 1, p. 301-317.

Brown, T. H., ms, 1970, Theoretical predictions of equilibria and mass transfer in the system CaO–MgO–SiO_2–H_2O–CO_2–$NaCl$–HCl: Ph.D. dissert., Northwestern Univ., Evanston, Ill.

Bryan, W. B., Finger, L. W., and Chayes, F., 1969, A least-squares approximation for estimating the composition of a mixture: Carnegie Inst. Washington Year Book 67, p. 243-244.

Burnham, C. W., Holloway, J. R., and Davis, N. F., 1969, Thermodynamic properties of water to 1000°C and 10,000 bars: Geol. Soc. America Spec. Paper 132, 96 p.

Chayes, Felix, 1951, Modal analyses of the granite and diabase test rocks: U.S. Geol Survey Bull. 980, p. 59-68.

Chinner, G. A., 1960, Pelitic gneisses with varying ferrous/ferric ratios from Glen Clora, Angus, Scotland: Jour. Petrology, v. 1, p. 178-217.

Clarke, F. W., 1924, Data of geochemistry: U.S. Geol. Survey Bull. 770, 841 p.

Cross, W., Iddings, J. P., Pirsson, L. V., and Washington, H. S., 1903, Quantitative classification of igneous rocks: Chicago, Ill., Univ. Chicago Press, 286 p.

Darken, L. S., and Gurry, R. W., 1953, Physical chemistry of metals: New York, McGraw-Hill, 535 p.

Duhem, P., 1899, Traite elementaire de mechanique chimique: Paris, A. Hermann et fils, v. 4, 384 p.

Fisher, J. R., and Haas, J. L., 1973, Simultaneous evaluation and correlation of thermochemical data [abs.]: Am. Geophys. Union Trans., v. 54, p. 482.

Frey, Martin, 1969, A mixed-layer paragonite/phengite of low-grade metamorphic origin: Contr. Mineralogy and Petrology, v. 24, p. 63-65.

Gordon, T. M., 1973, Determination of internally consistent thermodynamic data from phase equilibrium experiments: Jour. Geology, v. 81, p. 199-208.

Helgeson, H. C., 1969, Thermodynamics of hydrothermal systems at elevated temperatures and pressures: Am. Jour. Sci., v. 267, p. 729-804.

Kelley, K. K., 1960, Contributions to the data on theoretical metallurgy XIII. High-temperature heat capacity, and entropy data for the elements and inorganic compounds: U.S. Bur. Mines Bull. 584, 232 p.

Prigogine, I., and Degay, R., 1954, Chemical thermodynamics, translated by D. H. Everett: London, Longmans Green, 543 p.

Robie, R. A., 1966, Thermodynamic properties of minerals, *in* Clark, S. P., Jr., ed., Handbook of physical constants: Geol. Soc. America Mem. 97, p. 437-458.

Robie, R. A., and Waldbaum, D. R., 1968, Thermodynamic properties of minerals and related substances at 298.15°K (25.0°C) and one atmosphere (1.013 Bars) pressure and at higher temperatures: U.S. Geol. Survey Bull. 1259, 256 p.

Schlect, W. G., and Stevens, R. E., 1951, Results of chemical analyses of samples of granite and diabase: U.S. Geol. Survey Bull. 980, p. 7-24.

Thompson, J. B., 1967, Thermodynamic properties of simple solutions, *in* Abelson, P. H., ed., Researches in geochemistry, v. 2, New York, John Wiley, p. 340-361.

Van Zeggeren, F., and Storey, S. H., 1970, The computation of chemical equilibrium: Cambridge, England, Cambridge Univ. Press, 176 p.

Wright, T. L., and Doherty, P. C., 1970, A linear programming and least squares computer method for solving petrologic mixing problems: Geol. Soc. America Bull., v. 81, p. 1995-2008.

Zen, E-an, 1972, Gibbs free energy, enthalpy, and entropy of ten rock-forming minerals: calculations, discrepancies, implications. Am. Mineralogist, v. 57, p. 524-553.